



## Design and Process Considerations for a Tunneling Tip Accelerometer

*Paul M. Zavracky, Bob McClelland, Keith Warner and Neil Sherman  
Northeastern University  
360 Huntington Avenue  
Boston, MA 02115*

*Frank Hartley  
Jet Propulsion Laboratory  
4800 Oak Grove Drive  
Pasadena, CA 91190*

### Abstract

In this paper, we discuss issues related to the fabrication of a bulk micromachined single axis accelerometer. The accelerometer is designed to have a full scale range of ten mill g and a sensitivity of tens of nanog. During the process, three distinctly different die are fabricated. These are subsequently assembled using a alloy bonding technique. During the bonding operation, electrical contacts are made between layers. The accelerometer is controlled by electrostatic force plates above and below the proof mass. The lower electrode has a dual role. In operation, it provides a necessary control electrode. When not in operation, it is used to clamp the proof mass and prevents its motion. Results of the fabrication process and initial testing of the clamping function are reported.

### Introduction

In its simplest form, a conventional accelerometer consists of a proof mass, a spring and a position detector. Under steady state conditions, the proof mass experiencing a constant acceleration will move from its rest position to a new position determined by the balance between its mass times the acceleration and the restoring force of the spring. Using a simple mechanical spring, the acceleration will be directly proportional to the distance traversed by the proof mass from its equilibrium position.

In a force feedback approach, the position of the proof mass is held nearly constant. This is accomplished by feeding back position information to the control electrodes. In this work, we are exploring the application of electron tunneling tips as position sensors. The resolution of accelerometers is directly proportional to the position detection capability and the effective closed-loop spring constant. Our approach to ultrahigh resolution devices is to incorporate a weak spring with a sensitive position detector. For position sensing, an electron tunneling tip has been suggested<sup>1,2,3</sup>. Tunneling tips have been used in sensors with reported

resolution below  $0.001 \text{ \AA}/\sqrt{\text{Hz}}^{4,5,6}$ . However, until now there has been no means of fully protecting tips and delicate structures during handling under shock loading

A key element of our design is the placement of the tip such that the spacing between the neutral position of the proof mass and the top of the tip is zero. This has two beneficial effects. It reduces sensitivity to off-axis acceleration by eliminating torque. In this design, the springs are composed of beam sections. If the proof mass were not centered, the beams would be deflected. Lateral acceleration of the proof mass would then resolve into a normal and axial loads on the springs. The normal component would deflect the beam and proof mass further, thereby giving a false acceleration reading. In a similar manner, thermal effects due to changes in spring stiffness are also significantly reduced.

## II) Specifications

The basic concept for the accelerometer is derived from a need for higher sensitivity with low mass and small volumes suitable for space-based applications. Silicon micromachining techniques provided a potential method to fabricate a small accelerometer, but similar devices reported by others could not achieve the necessary sensitivity<sup>1,7</sup>. These devices had been based on either piezoresistive or capacitive position sensing elements. In this design, the use of an electron tunneling tip is fundamental to its superior performance. The basic design features include an electron tunneling tip position sensor, electrostatic force feedback control with pitch and roll capability, and high off-axis sensitivity.

Several important issues have been addressed in this design. To achieve the required sensitivity of  $10^{-8} \text{ g}$ , a large mass device with an extremely weak spring is required. The required mass is achieved by producing a relatively large ( $\sim 1 \text{ cm}^2$ ) bulk micromachined device in two separate wafers that are eutectically bonded together. Weak springs are fabricated by etching back the silicon to form  $25 \mu\text{m}$  thick diaphragms which are further patterned to form 2 cm long folded spring elements. A second issue is the minimization of off-axis sensitivity. This can be accomplished by insuring the proof mass when active is in the neutral axis of the springs. This requires that the tunneling tip is designed to be in near proximity ( $10 \text{ \AA}$ ) to the unperturbed

proof mass. It also requires that the spring system has only a single low frequency mode (in our case, 10 Hz) and that all other modes are widely separated. A third issue is that of tip protection. In this design, a single electrostatic force plate doubles as a parking electrode which is designed to attract and hold the proof mass in place using a low voltage ( $<15$  volts). Finally, all die used in the device are fabricated in silicon. This choice minimizes stresses that can arise from thermal mismatch. In addition, our bonding procedure is conducted at a low temperature ( $<400^{\circ}$  C) which permits bonding after the wafers have been processed through metal deposition. The bonding procedure also provides electrical interconnection for the device so that all bond pads are available from the top side of the completed accelerometer.

### 11) Layout

Figure 1 shows a cross section of the final device. This drawing is not to scale, but important features have been indicated. From this figure, we see that the design is based on a four wafer process. The four wafers will be bonded together and separated to produce the structure shown in the figure. Therefore, we can refer to four individual die that comprise the completed device. The top die in the figure is referred to as the tip die and the associated mask and wafer are referred to as the tip mask and wafer. The tip die has at its center an electron tunneling tip. The tip is approximately  $3.75\text{ }\mu\text{m}$  high. Two identical wafers rotated by  $90^{\circ}$  are bonded together to form the proof mass die. This die is comprised of a border region and the proof mass shown in the center of Figure 1. The proof mass will be  $1\text{ cm}$  ( $10,000\text{ }\mu\text{m}$ ) across. The lowest die is referred to as the force plate die. The proof mass is located in the exact center of the structure and the tunneling tip is designed to touch the proof mass. Figure 2 shows a top view of just the proof mass and springs and figures 3 and 4 show top views of the tip and force plate dice.

#### 3.1) Tip Die

Referring to figure 3, the tip die is the most complicated structure in the assembly. It not only incorporates the tunneling tip, but contains 4 field plates to control the pitch and roll of the proof mass as well as its position. The tip die must also accommodate the bonding method used to assemble the four separate die that comprise the accelerometer. In order to create the tip die, two separate metal layers are required. The first layer is isolated from the second by a  $0.5\text{ }\mu\text{m}$  oxide layer. The first metal layer is used for interconnecting the tip and quadrature plates to their associated wire bond pads. We are currently using chrome which survives a

subsequent LTO deposition process. This metal layer covers the tip and can be used as the tip metal. Chromium tips have been tested successfully.

The second metal layer is Cr/Au. It forms the quadrature plates and covers the electrical bond pads. It also forms a base layer for the eutectic bond ring that surrounds the center of the die. The center region of the die is recessed with respect to the bond ring and bond pads. This is required to obtain a spacing between the field plates and the proof mass. When this die is bonded to the proof mass, the perimeter will form a hermetic seal and the bond pads will be mechanically bonded and electrically connected to their counterparts on the proof-mass die. This electrical connection scheme is a key feature of the design. By interconnecting the die in the bonding processes, all electrical connections to the completed accelerometer can be made from its front surface.

The lower right hand corner of Figure 3 shows a magnified section of the tip. This illustrates the relationship of the tip to the bond perimeter and illustrates the two metal layer design. As can be seen, the electrically insulating oxide layer is removed from the tip and its surrounding area, exposing the tip metal.

The electrical contact to the tip is accomplished with the first metal layer which is connected by a single thin lead to the bond pad. The second metal layer which forms the field plates, bond perimeter and wire bond pads is deposited above the first metal layer. Focusing on the center of the die, the figure shows a cross centered in the bond perimeter which is electrically grounded. It is used to shield the tip metal lead from electric fields that exist in the vicinity of the field plates. In the upper right hand corner of Figure 3 a detail of the center of the cross is shown. The cross is open at the very center to expose the tip below. At the end of the tip wafer process, metal can be selectively deposited on the tip allowing flexibility in the choice of tip metal.

Not shown in the figure is the exact nature of the first metal layer. It is patterned in such a way it underlies the center cross region. This maintains the electrostatic symmetry of the device. Therefore, the tip metal layer is sandwiched between the wafer and the second metal layer. Silicon oxide is used to isolate the tip metal from both the substrate and the second metal. Because the tip metal also underlies the four electrostatic control plates, the second metal layer is at the same elevation at the cross as it is at the control plates.

To connect the force plates electrically to the bond pack, holes are cut in the oxide layer above the first metal in the vicinity of the force plates. This allows the force plates to contact the first metal layer. The first metal layer is patterned in such a way as to connect each force plate electrically to its associated bond pad. The bond pads also contain a connection between first and second metal as shown in the details to the left of Figure 3.

Finally, a bond metal layer is deposited and patterned on the bond perimeter. The bond perimeter is also recessed, but not as deeply as the quadrature plates. This recess implements a surface referenced bonding technique we are using. The concept is that the width of the bond metal ring is less than the underlying chrome/gold layer, but its thickness is greater than the depth of the recess. When bonding, the eutectic alloy wets both parts and draws them together through surface tension.

### 3.2) Proof Mass Die

Figure 1 shows a cross-section of the proof mass die. The proof mass is assembled from two identical die. As a result of the anisotropic etchant used to machine the proof mass, its sides will be tapered at  $54.7^\circ$ . Since the wafer is  $400\text{ }\mu\text{m}$  thick, the smallest dimension of the proof mass will be two times  $253.2\text{ }\mu\text{m}$  smaller than the top surface or  $9433.6\text{ }\mu\text{m}$ . The top dimension is  $1\text{ cm}$  or  $10,000\text{ }\mu\text{m}$ . The volume of silicon lost to this undercutting is approximately  $4.5 \times 10^{-3}\text{ cm}^3$ . The volume of a box  $1\text{ cm} \times 1\text{ cm} \times 800\text{ }\mu\text{m}$  is  $8 \times 10^{-2}\text{ cm}^3$ . Since the density of silicon is about  $2.42\text{ g/cc}$ , the net weight of the proof mass is the difference of the two volumes above times the density or  $0.18\text{ gm}$ . The proof mass is held to the surrounding frame by a set of springs referred to as 'crab legs'. In figure 1, the target thickness of the crab legs is  $25\text{ }\mu\text{m}$ . Figure 2 shows a top view of the proof mass and springs. The detail on the left of the figure gives the spring width, separation and thickness.

Each individual crab leg is divided into three spring sections, two short ones and one long one. The length of the short sections is  $5000\text{ }\mu\text{m}$  but the length of the long spring deviates by  $200\text{ }\mu\text{m}$  from  $10,000\text{ }\mu\text{m}$  due to the requirement to clear the corner ties. The corner ties play no role in the normal motion of the proof mass and

do not alter the stiffness of the device in its sensitive axis. These ties are added to increase the stiffness to pitch, roll and yaw<sup>9</sup>

The proof mass die is maintained at essentially ground potential and the surface of the proof mass is completely covered by metal. However, at the perimeter of the die, electrical contact between bond pads is routed to facilitate the front surface only contacting scheme described above. Figure 5 shows the metal layer layout for the proof mass. Since the anisotropic etching can take place prior to metallization, some freedom exists in the choice of proof mass metal. Our intention is to provide a complimentary layer to the one used on the tip and force plate chips.

The bonding of the proof mass wafers requires special attention. In this case, the bond metal (assuming eutectic bonding is to be used) is applied to the back side of the wafer. If the bond metal is applied early in the process, it must survive all subsequent processing steps. This puts a severe and unnecessary restriction on the choice of bond material. Applying the bond metal at the end of the process, prior to cutting the springs is the preferred method. Two patterning techniques have been employed. Since the back side to the wafer has been deep etched, photolithographic patterning is difficult, but we found, not impossible. Double spinning a thick resist such as Shipley's 1827 is effective. Resist accumulated in the lower corners of etch pits is removed after a long exposure (5 min at 40 row). This technique preserves the hermetic sealing capability we desire. Alternatively, this layer can be deposited through a shadow mask. Both methods have been used successfully.

### 3.3) Force Plate Die

The force plate die is in many ways similar to the tip die. Again a two metal process is used in order to provide a bond perimeter which is not electrically connected to the force plate. A contact pad to this perimeter metal is provided in order to set the potential. The force plate is fabricated in first metal which may simply be a single chrome layer similar to that used on the tip wafer. The force plate must be covered with a thick oxide layer (1 $\mu$ m). The purpose of this oxide layer is to prevent an electrical contact between the proof mass and the force plate when the proof mass is being clamped electrostatically. Choices for the bond perimeter and contact layer (second metal) are identical to those described for the tip wafer

#### IV) Assembly

Figure] shows drawing of the cross-section of the assembled accelerometer die. In particular, the nature of the bond pad regions is illuminated. Since the bond pads are meant to contact metal lines on the tip die as well as the force plate die, it is necessary to access bond pads on the force plate and tip dice. To the top right of the figure, an etched groove is shown extending down to the top of the first proof mass die. Contacts to the tip and control plates are made at this level. On the extreme left side of the assembled die, a complex anisotropically etched hole extends down to the force plate wafer. Bond pads for the force plate and its ground are made through openings of this kind. Referring again to figure 5 which shows the top of the proof mass, 'dog bone' interconnections are shown. Wire bonds are made to one side of each interconnection through the anisotropically etched grooves. The five required electrical connections to the tip wafer are made to the opposite end of each interconnection during the eutectic bonding process. Therefore, the pads seen on the tip wafer are connected to the interconnections on the proof mass via the eutectic bonding. The opposite side of each interconnection is accessible through an etched groove for wire bonding. The force plate die has only two electrical connections, one to the force plate itself and another to the bond ring. Both are accessible through deep anisotropic grooves. The bond ring makes electrical connection to the proof mass via the eutectic bonding process. Substrate contacts are currently being made at the periphery of the die during the packaging process.

#### V) Results

Fabrication of devices has revealed several important issues that must be addressed to successfully complete the device. Our initial work on wafer bonding was performed with Aluminum Germanium alloys. Layers were deposited in an e-beam evaporator and the thicknesses were adjusted to provide the eutectic alloy when both layers combined. Although the eutectic alloy should melt at 450 °C, reliable bonding did not occur until 500 °C. After bonding the proof mass wafers, it became apparent that the TiW/Au layers on the proof mass had degraded. While the degradation appeared to be minor, we found that the films developed a built-in strain. The effect of the strain manifest itself in bending of the springs out of plane. Experimentation with springs annealed at various temperatures revealed a safe temperature range of 350 °C and below. We subsequently changed the eutectic bonding system to Iridium alloys.



Full accelerometers have been fabricated. Figure 6 shows a top view of an assembled accelerometer where the corner of the tip die has been broken away revealing the proof mass beneath. For test purposes we have assembled devices in three stages, full, three quarter and on half. A three quarter accelerometer is one which has both bonded proof mass die and the force plate. A one half accelerometer consists of a single proof mass die and a force plate.

After assembling the first accelerometers, we found that the voltage required to hold the proof mass in place against 1g was much higher than expected. The typical value is about 3 volts compared to a calculated value of about 0.6 volts. Measurements of the capacitance showed that instead of the expected 3 nanofarads, the actual capacitance was approximately 300 picofarads. These results suggested that either foreign matter prevented the proof mass from coming into full contact with the force plate, or the proof mass and force plate do not conform to one another. To test the latter theory, we ran surface profiles of the proof mass and force plates. Measurements indicated that as much as 10 microns of variation are typical on proof masses. Tests of starting material produced similar results. This suggests that either higher voltages are required to implement the parking procedure effectively, or that wafer specifications must be improved.

To develop an understanding of the magnitude of this problem a simple model of the proof mass and force plate was created. This model assumed that the proof mass had a radius of curvature,  $R$ . Based on this spherical model, the electrostatic potential required to generate a force of 1 g between the force plate and the proof mass, with the proof mass in contact with the dielectric layer at its center was calculated. Figure 7 shows the configuration considered. The problem was modeled numerically and showed that if the proof mass had a radius of curvature of about 100 cm, then 'd' would be about 10 pm, the capacitance would be about 350 picofarads, and it would require 3.3 volts to support the proof mass against 1g. These results are consistent with our observations.

The proof mass is held to the force plate by an electrostatic potential. To prevent shorting, the force plate has been covered with a low temperature oxide (LTO) layer. It has been suggested that if a DC field is applied, an

opportunity for charging of the insulator surface exists and that the voltage required to hold the proof mass against 1 g would increase in time. To test this hypothesis, we have experimented with electrically stressing the silicon dioxide. A half accelerometer is connected to an LCR bridge with DC bias capability. The accelerometer was oriented such that the proof mass rested on the force plate. A DC bias of about 5 volts was applied. The unit was flipped over and the DC field reduced while monitoring the capacitance until the applied field could no longer hold the proof mass against the force plate. At this point, the capacitance changes abruptly. A bias voltage of 2.7 volts was recorded. The device was then flipped over again, and a 10 volt bias was applied. This was held constant for periods up to 24 hours after which the holding voltage was again measured. We observed a slight reduction (50 mv) of the potential required to hold the proof mass which may be attributed to charging of the silicon dioxide.

Although minimal charging has been observed, a means to completely obviate this issue is desirable. In our work, we have been experimenting with the application of AC voltages. Tests with AC fields have proven successful in countering surface charging. Most of our work has been conducted with sinusoidal sources, with the unfortunate drawback that the peak voltage must be  $\sqrt{2}$  the value of a DC field with equivalent holding power. AC fields add a new dimension of flexibility that can be exploited for MEMS. With an AC applied field, a capacitor can be placed in series with the device, limiting current flow. In an extreme case, a small series capacitor will behave like a constant current source. Since the electrostatic force applied is proportional to the square of the current and independent of the spacing, an AC field can be used to apply a position independent force to a moving micromechanical device. A second interesting aspect of AC fields is that they can be used simultaneously for the measurement of position and for control. In our work, we have successfully exploited AC fields to position the proof mass.

### Conclusions

We have reported a new fabrication process and configuration for an ultrasensitive accelerometer. The accelerometer is fabricated using a bulk micromachining approach. Three unique dies are processed and bonded together to form the final device. The bonding process, which uses eutectic alloys, joins the die and simultaneously provides hermetic sealing and electrical interconnection between die. The accelerometer is

designed with a force plate that can be used to hold delicate proof mass and spring assembly electrostatically during transportation. It has been determined that concerns about charging of the silicon oxide layer deposited on the force plate are minor. Changes in the holding potential of only about 50 millivolts have been observed. This issue can be negated through the use of AC rather than DC electrostatic fields. These have been demonstrated successfully.

### **Acknowledgments**

The authors would like to acknowledge the help and support of Greg Jenkins for his assistance in fabricating devices and Professor Nick McGruer for his many helpful suggestions. Funding for this program has been provided by NASA through a grant to the Jet Propulsion Laboratories.

## References

- 1 AA. Braski, T.R. Albrecht, and C. F. Quate, "Tunneling Accelerometer," J. Microscopy, Vol. 152, p. 100, 1988.
- 2 S.B. Waltman and W. J. Kaiser, "h Electron Tunneling Sensor. " Sensors and Actuators, Vol. 19, pp 201-210, 1989.
- 3 M.F. Bocko, "The scanning tunneling microscope as a high-gain, low noise displacement sensor," Rev. Sci. Instrum. Vol. 61, No. 12, December 1990.
- 4 T.W. Kenny, W.J. Kaiser, H K. Rockstad, J.K Reynolds, J.A Podosek, and E C Vote, "Wide-Bandwidth Electromechanical Actuators for Tunneling Displacement "transducers," J. MEMS, Vol. 3, No. 3, September 1994.
- 5 T.W. Kenny, W.J. Kaiser, S.B. Waltman, and J.K. Reynolds, "A Novel Infrared Detector Based on a Tunneling Displacement Transducer," Appl. Phys. Lett, Vol. 59, 1991.
- 6 J.J. Yao, S.C. Arney, N.C. MacDonald, "T'abdication of High Frequency Two-dimensional Nanoactuators for Scanned Probe Devices," J. MEMS, Vol. 1, No 1, pp. 14-22>1992.
- 7 E. Peeters, S. Vergote, B. Puers and W. Sansen, "A highly symmetrical capacitive micro-accelerometer with single degree of freedom response.," J Micromech Microeng Vol. 2, pp. 104-112, 1992
- 8 P.M Zavracky, F. Hartley, N. Sherman, T. Hansen, and K Warner, "A New Force Balanced Accelerometer using Tunneling Tip Position Sensing," 7th Int. Conf. on Sensors and Actuators, Yokahama, Japan, June 7-10, 1993.
- 9 P.M. Zavracky, F. Hartley, and D Atkins, "New Spring Design and Processes for an Electron Tunneling Tip Accelerometer, to be published
- 10 P. M. Zavracky and Bao Vu, "Eutectic Bonding with Al/Ge Thin Films," to be published.

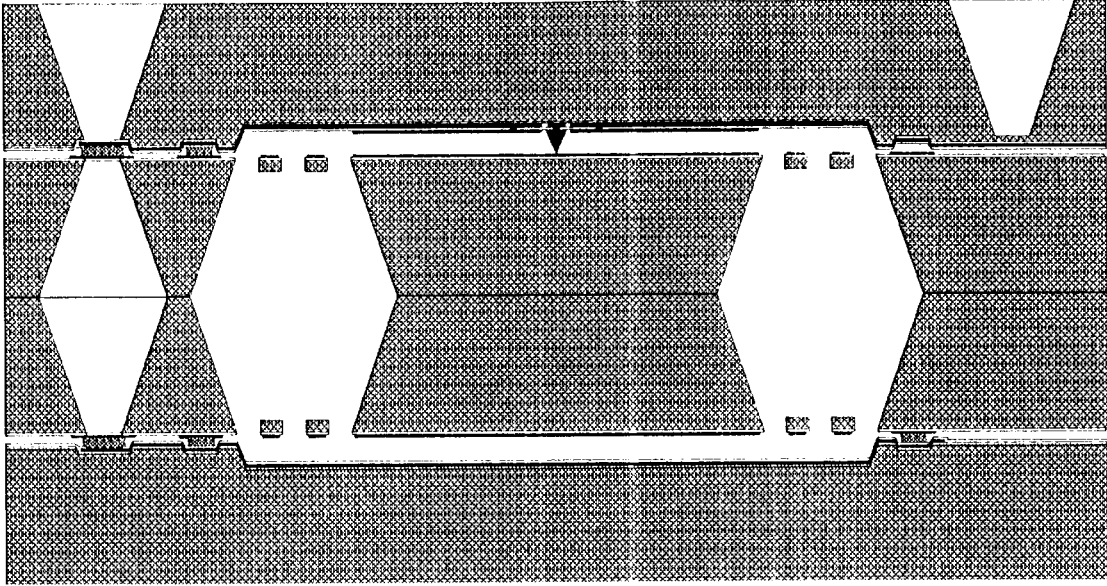


Figure1. Cross-section of an assembled accelerometer.

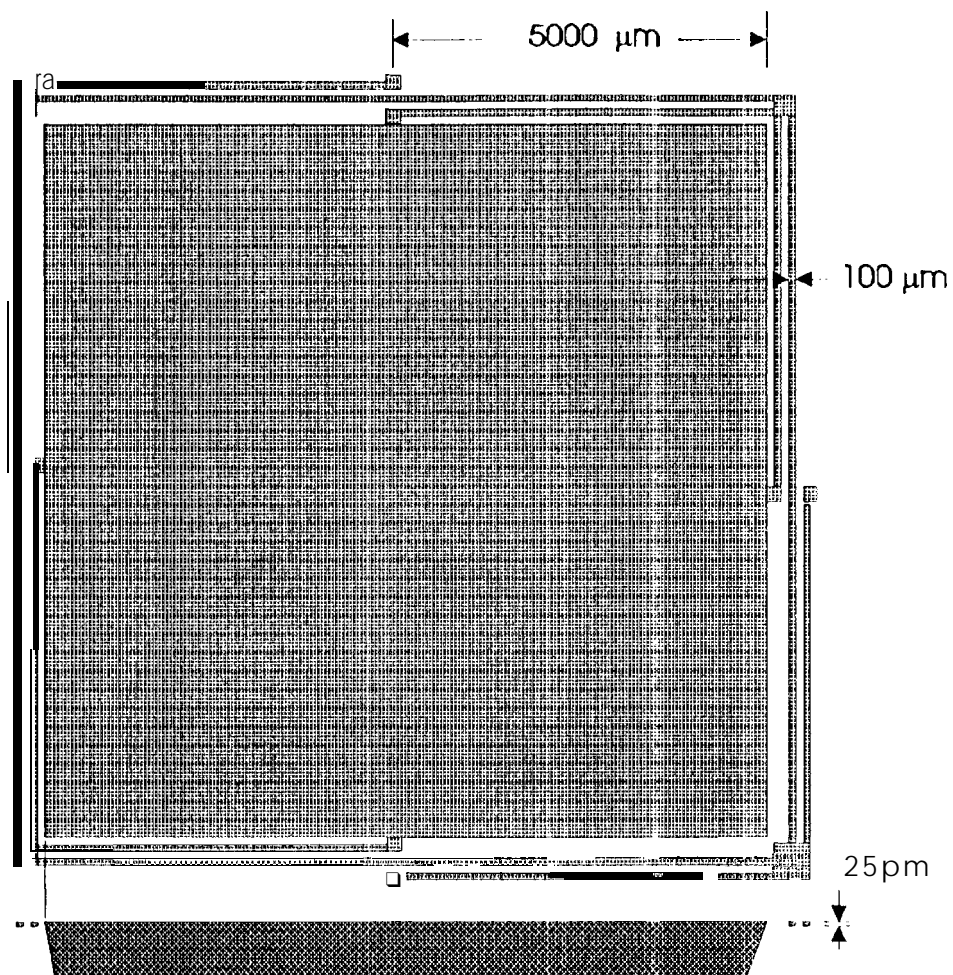


Figure 2. a) A top view of the proof mass and spring assembly. b) a cross-section of the same

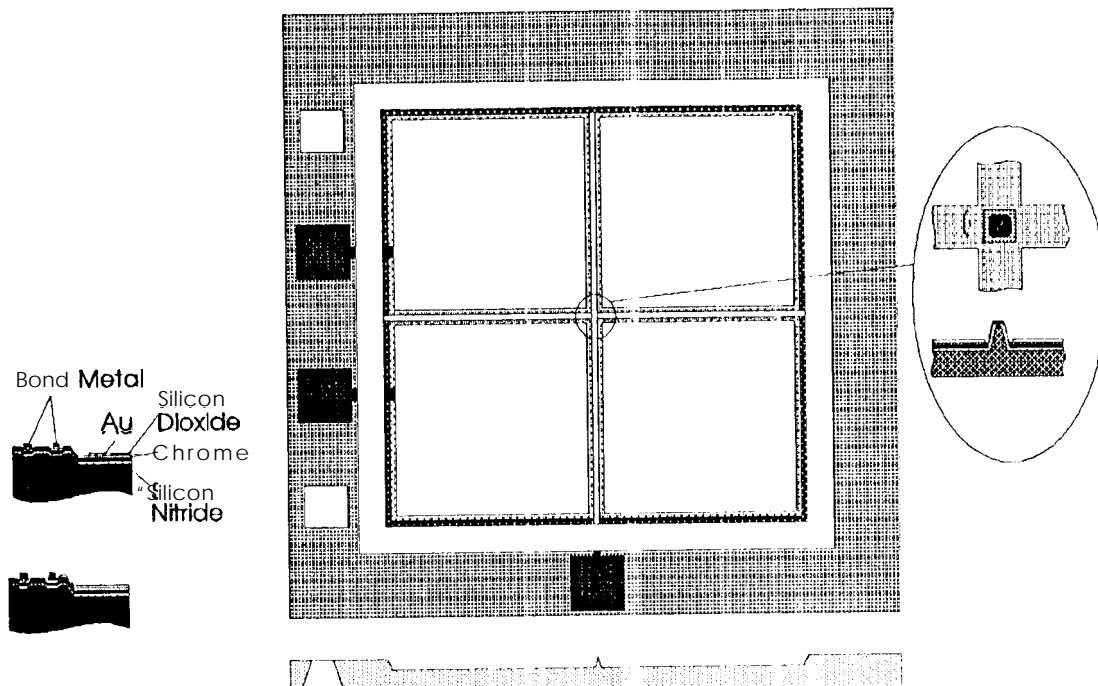


Figure 3. Various views of the tip die. The tip is located in the very center of the device. A single shielded electrical lead provides continuity between the tip and its associated wire bond pad. The four quadrant plates surrounding the tip can be used to control pitch and roll. Surrounding the four quadrant plates is a eutectic bond ring.

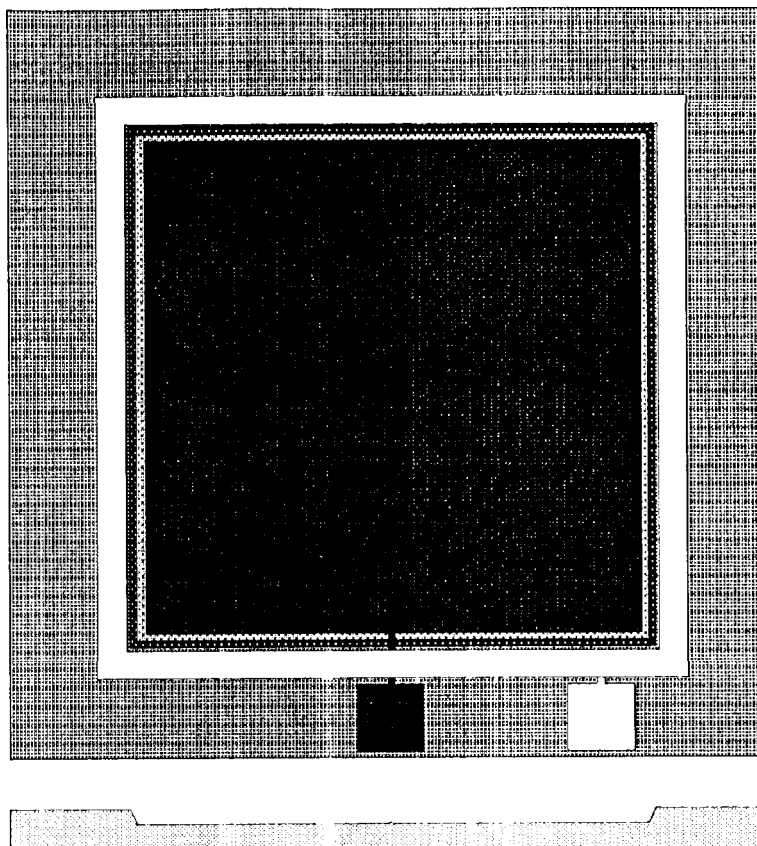
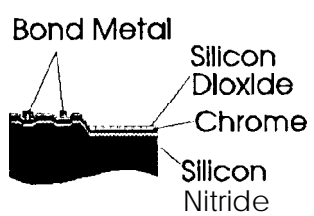


Figure 4. Various views of the force plate die. The center region contains an oxide covered force plate. A first metal forms the force plate, lead and wire bond pad. Surrounding the center depression and force plate is a eutectic bond ring.



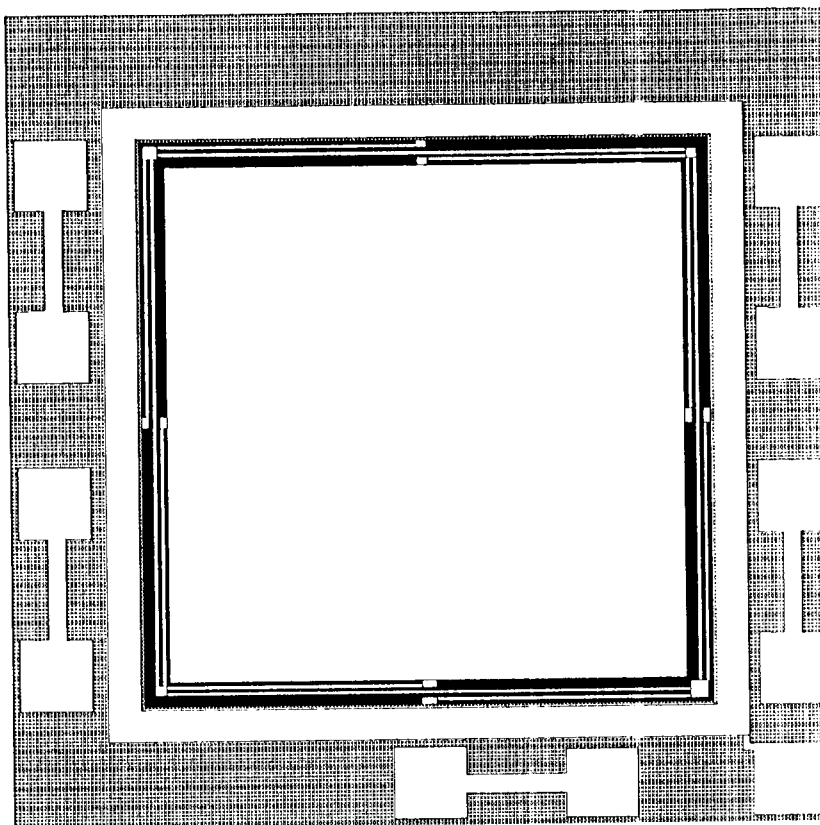


Figure 5. Metal layout on the proof mass die. The dog bone structures are used to provide front surface access to all contacts in the assembled device.

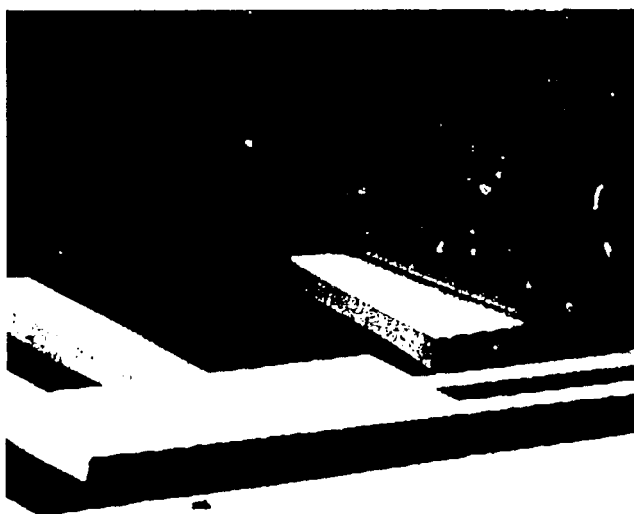
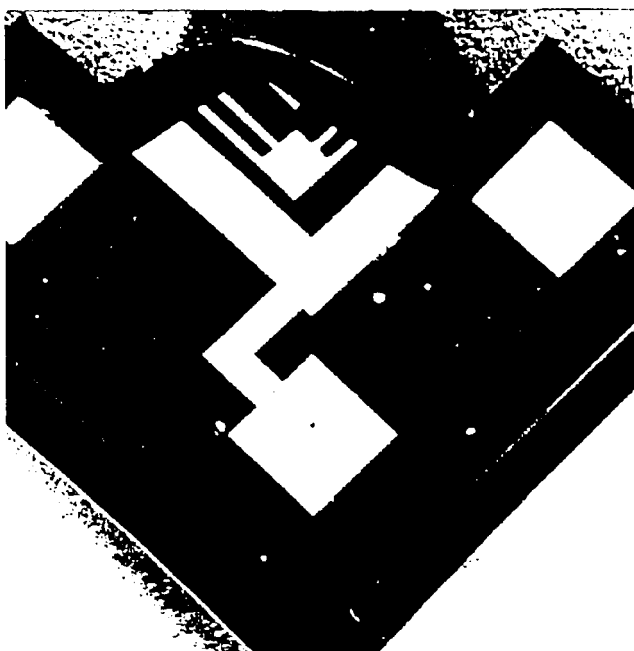


Figure 6. a) Top view of completed accelerometer with tip die cut away to reveal the internal structure using an SEM b) Close up view showing the 10 mm gap between the proof mass and tip quadrant plates.

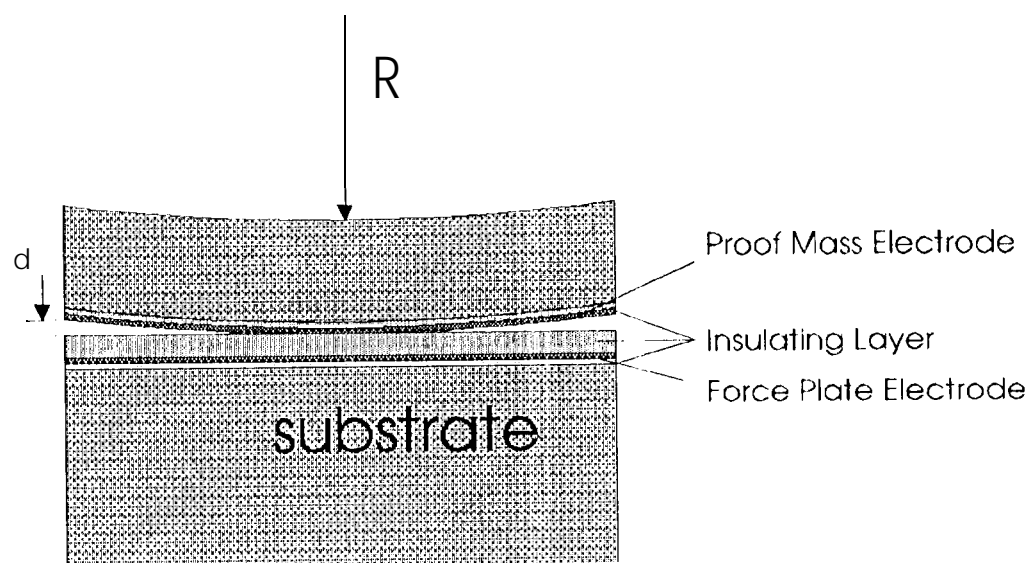


Figure 7. Possible cross-section of the proof mass resting on the force plate